Hindawi Publishing Corporation
ISRN Renewable Energy
Volume 2013, Article ID 851876, 8 pages
http://dx.doi.org/10.1155/2013/851876

Research Article

Carbon Based PV: n-Si(100)/DLC Structure for Photovoltaic Application

D. Ghosh,[1] B. Ghosh,[1] Anindita Ghosh,[1] S. Hussain,[2] R. Bhar,[1] and A. K. Pal[1]

[1] *Department of Instrumentation Science, USIC Building, Jadavpur University, Calcutta 700 032, India*
[2] *UGC-DAE CSR, Kalpakkam Node, Kokilamedu 603104, India*

Correspondence should be addressed to A. K. Pal; msakp2002@yahoo.co.in

Received 25 June 2013; Accepted 5 August 2013

Academic Editors: E. Kymakis and P. D. Lund

Diamond-like carbon films were electrodeposited on n-Si substrate to realize an n-Si/DLC PV structure. The films thus obtained were characterized by FESEM, XPS, FTIR, and Raman studies. Solar cell characteristics were also investigated critically. Maximum efficiency of 3.7% was obtained for the best n-Si(100)/DLC structure. Carrier life time was obtained from V_{oc} decay measurement. It was observed that photoinduced charge separation in n-Si(100)/DLC structure was associated with an increase in the dielectric constant and a decrease in the device resistance. The process, being reproducible, cheap, and scalable, involving significantly less process steps, is likely to usher a new hope to the current competitive scenario of PV technology.

1. Introduction

During the last two decades diamond-like carbon (DLC) films were studied extensively due to their fascinating and exotic properties. Reports on the microstructural, mechanical, electrical, optical, and thermal properties of hydrogenated amorphous carbon films have poured in the literature [1–7]. Along with these properties and being a p-type material, DLC films are emerging as a potential candidate for photovoltaic application [8–11]. Although different carbon nanostructured materials showed promises in this regard, difficulty in depositing diamond-like carbon films directly on silicon substrates [12, 13] adopting cost-effective, scalable, and reproducible technique deterred the use of such carbon materials for device application. In recent times, Paul et al. [14] studied hydrophobic characteristics of such DLC films deposited on SnO_2-coated substrates while Gupta et al. [15] reported the dependence of field emission properties of DLC films electrodeposited at different voltage. Although there has been intense research activity on the use of carbon nanomaterials in areas such as electronics and photonics [16], the use of carbon in various forms as the active layer material in PV is still largely unexplored. Moreover, the use of carbon nanostructured materials would favour the use of green technology in PV cell manufacturing areas. Recent reports indicated the use of carbon materials mainly in photovoltaics as acceptors in polymer-based solar cell or as transparent electrodes [8] and only recently as the main active layer components in polymer free solar cells [9, 17, 18]. In this paper, the viability of utilizing electrodeposited DLC films on n-Si (100) for PV application is explored.

2. Experimental Details

Diamond-like carbon films (DLC) were synthesized by electrolysis using acetic acid (CH_3COOH) and deionized water as electrolyte. The substrates used in this study are n-type single crystal silicon (100) wafers (0.3 mm thick) doped with phosphorus. The resistivity of the silicon substrates was ~1–5 Ω-cm. Electrolysis was carried out at atmospheric pressure and the bath temperature was kept at ~300 K. The silicon substrate (~10 mm × 8 mm × 0.3 mm) was attached to a copper cathode. Graphite was used as the counter electrode (anode). Before mounting the substrates on the cathode, they were etched with a solution of deionized water, hydrofluoric acid, and nitric acid in the ratio of 5 : 1 : 1 and then rinsed with deionized water. It was finally ultrasonically cleaned using

isopropyl alcohol. The electrodes were separated by a distance of ~8 mm. The applied voltage between the electrodes was kept ~16 V by using a d.c. power supply capable of generating stabilized voltage (30 V, 2 A). A pH meter was used to maintain the pH of the bath at ~4 throughout the experiment. Details of deposition techniques are available in our earlier publication [12, 13]. The films were deposited at 16 V in baths containing three different amounts (1%, 4%, and 8% v/v) of CH_3COOH in water. The deposition time was kept at 60 min, and films thickness, as measured by stylus method, varied between 300 to 500 nm. Indium and gold were deposited by thermal evaporation as back and top contacts, respectively, for characterization.

The surface morphology of the films was studied by field emission scanning electron microscope (FESEM) (Carl Zeiss SUPRA 55 with GEMINI technology). FTIR spectra were recorded in the range of 400–4000 cm^{-1} by using a Nicolet-380 FTIR spectrometer. Raman spectra were recorded using Renishaw in via micro-Raman spectrometer using 514 nm Argon laser. X-ray photoelectron spectroscopy (XPS) measurements were carried out using an M/s SPECS (Germany) make spectrometer at a system pressure of ~ $4e-10$ Torr. Al Kα line was used as the X-ray source at 1486.74 eV.

3. Results and Discussion

In the CVD technique utilized for the deposition of various carbon nanostructures, methane and hydrogen gas mixtures were generally used as a precursor gas. This resulted in the formation of CH_3^+ radicals along with hydrogen ions and electrons in the plasma which took part in the making and breaking of bonds to produce different carbon nanostructures during growth on the substrates. Nature of hybridization of the carbon atoms forming the nanostructure depended on the relative amount and energy of CH_3^+ radicals and hydrogen ions impinging on the substrate. In the electrodeposition technique described here, CH_3^+ radicals dissociated from CH_3COOH are the source of carbon. Additionally, hydrogen ions available from the electrolysis process in the bath containing CH_3COOH and deionized water would also take part in the making and breaking of the bonds to produce amorphous carbon in the form of very small clusters with unsaturated dangling bonds. The nature of the substrate, especially Si, would also play a significant role in terms of providing anchorage to the above ions/radicals. The dangling bonds at the surface of Si substrates used would serve the purpose. The effect of doping with phosphorous on the modulation of dangling bonds associated with the Si substrates has been extensively studied by Yang et al. [19].

The acetic acid in water would tend to ionize and be transported in the electrolyte under an electric field as:

$$\begin{gathered} CH_3COOH + H_2O \longrightarrow CH_3^+ + (COOH)^- + H^+ + (OH)^- \\ CH_3^+ + CH_3^+ + 2e \longrightarrow CH_2 = CH_2 + H_2 \\ nCH_2 = CH_2 \longrightarrow [-CH_2CH_2-]_n. \end{gathered} \tag{1}$$

One would expect the presence of very high concentration of methyl radicals and hydrogen ions at the cathode surface, are during electrolysis. Thus, the basic requirements for depositing diamond or DLC films, that is, presence of large concentration of methyl radicals and hydrogen ions at the substrate surface is satisfied. Dangling bonds at the n-Si substrate surface would provide anchorage to the CH_3^+ radicals along with H^+ which would take part in breaking and making of sp^2 and sp^3 bonded carbon, respectively, to ensure the growth of DLC film.

3.1. Microstructural and XPS Studies. Figures 1(a) and 1(b) show the field emission scanning electron micrographs (FESEM) of two representative DLC films deposited in a bath containing two different amounts of acetic CH_3COOH (1% and 8% v/v) on n-Si substrates. It may be noted here that microstructures of the DLC films deposited here did not differ significantly. The films are quite compact with well-defined grains covering the whole silicon surface. The grain size decreased for films deposited with increased CH_3COOH concentration. The corresponding histograms (shown in the insets of Figures 1(a) and 1(b)) indicate a narrow distribution of grains. The average grain size slightly decreased from 20 nm to 18 nm as the concentration of CH_3COOH was increased from 1% to 8%. The films deposited from a bath containing 1% v/v CH_3COOH are the most compact ones and had better uniformity in grain size distribution than those deposited with higher amount of CH_3COOH in water.

Figure 1(c) shows the XPS spectra of a representative film deposited on n-Si substrates in a bath containing 1.0% CH_3COOH. The spectra indicated the presence of carbon and oxygen only. Presence of oxygen in the XPS spectra may be either due to physisorbed oxygen acquired during exposure to ambient and related formation of surface oxide phases or to the OH radicals acquired from the aqueous bath. Using the standard XPS atomic sensitivity factors for C 1 s (0.25) and O 1 s (0.66), the atomic ratio of C : O as determined from peak height measurements was 5 : 1.

3.2. FTIR Studies. The n-Si substrates used here were not transparent in the IR region and as such FTIR spectra of the DLC films deposited here could not be recorded in the transmission mode. FTIR spectrum recorded in the reflection mode in the range of 4000 and 400 cm^{-1} for a representative DLC film deposited in a bath containing 1.0% CH_3COOH is shown in (Figure 2(a)). One may observe that the spectra are dominated by the presence of peaks at ~679 cm^{-1}, 1591 cm^{-1}, and 2784 cm^{-1}. The peak at ~679 cm^{-1} could be identified as arising due to Si–Si bonds while the two small peaks at ~458 cm^{-1} are due to rocking modes of Si–O–Si bonds. The two peaks at ~1591 cm^{-1} and 2784 cm^{-1} could be identified as arising due to olefinic sp^2 C=C stretching modes and C–H stretching vibrations (two bands), respectively which are the only two peaks related to the DLC coatings [20]. The strong peak at 2360 cm^{-1} (Figure 2(a)) may be assigned to IR active O–C–O antisymmetric stretching bonds originating from the CH_3COOH bath fluid [21].

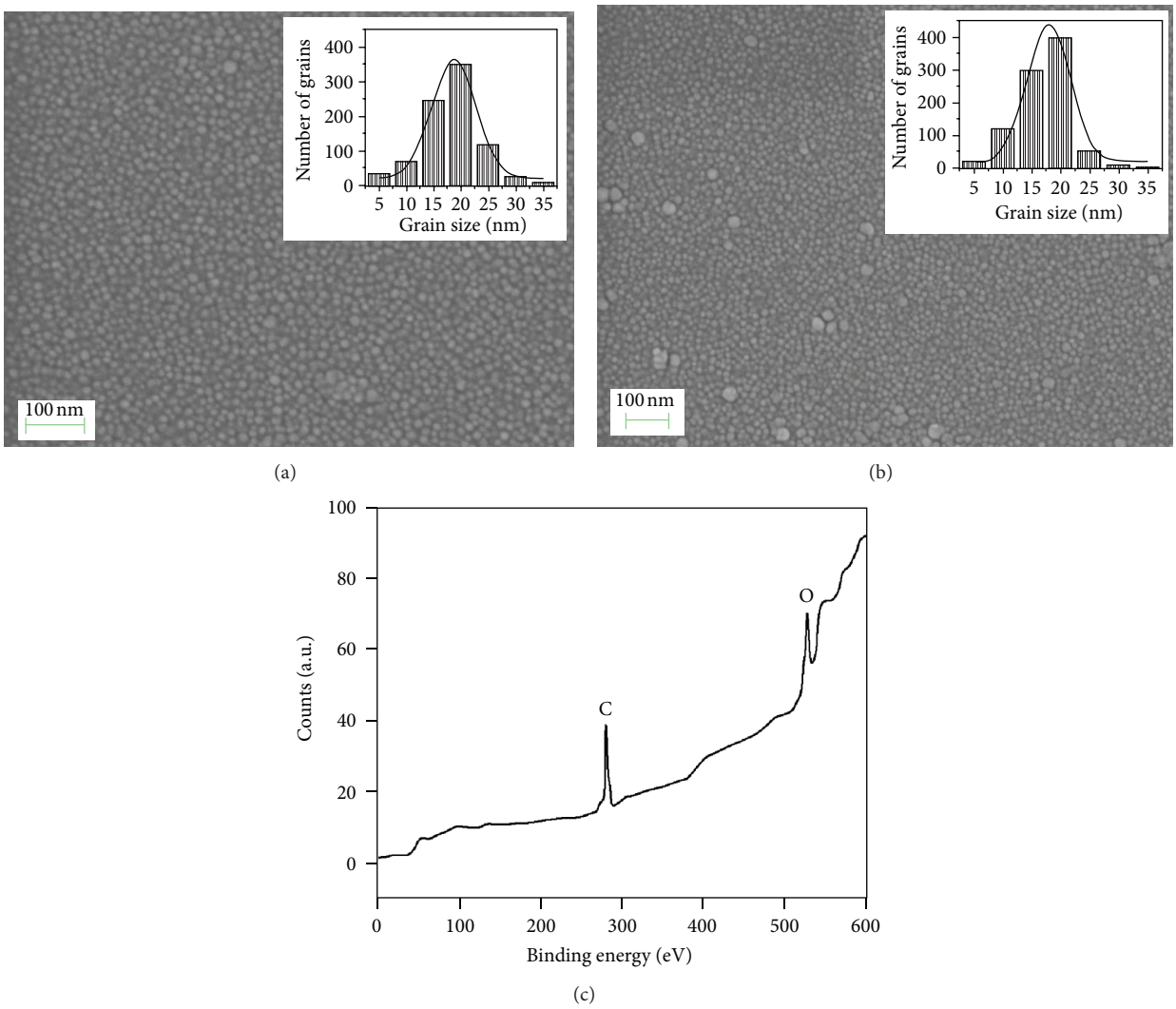

Figure 1: Field emission scanning electron micrograph (FESEM) of a DLC film deposited in a bath containing (a) 1.0% and (b) 8% (v/v) CH_3COOH on n-Si (100) substrates. Insets of (a) and (b) show the corresponding histograms. (c) XPS spectra of a representative film whose micrograph has been shown in (a).

3.3. Raman Studies. Raman spectra for a representative DLC films deposited in baths containing 1% CH_3COOH by volume which are shown in Figure 2(b) indicated the presence of two broad peaks, located at 1365 cm^{-1} (D-line) and 1575 cm^{-1} (G-line). It was observed that the position of the G-line shifted to higher wave number for films deposited in bath containing increased the amount of CH_3COOH in the bath. Unlike glassy carbon, the films are high resistive (>10 MΩ) reconfirming the nature of deposit being DLC.

It is well known that diamond has face-centered cubic symmetry. This would result in a triply degenerate first order phonon. The wave vector of the incident radiation is also much smaller than the Brillouin zone extension. Thus, the first order Raman peak at 1332 cm^{-1} is the diagnostic of the presence of diamond in carbon films. The structure of graphite would lead to two lattice vibrations resulting in Raman scattering at 42 cm^{-1} and 1581 cm^{-1} (the G-line). With increasing disorder, the peak ~1332–1365 cm^{-1} (D-line) may appear, and the intensity and width would increase with the decrease in microcrystalline domain size. The wave number of G-line would increase due to breakdown of the selection rule [22]. The sp^2 hybridized (π bonds) carbons having larger Raman scattering cross-section are more polarizable than the sp^3 hybridized (σ bond) carbon. Thus, the Raman spectra of DLC films would display both the D and G bands with larger peak widths. G-peak is a measure of the presence of sp^2-bonded carbon in all possible forms while D-peak is a measure of the presence of 6-fold ring structure in the visible Raman spectra of such materials for sp^3-bonded carbon.

3.4. Cell Characteristics

3.4.1. J-V and C-V Measurement. The DLC films deposited by this electrodeposition technique behaved like a p-type semiconducting material as observed by hot-probe technique. Thus, it would form a p-n junction with n-Si.

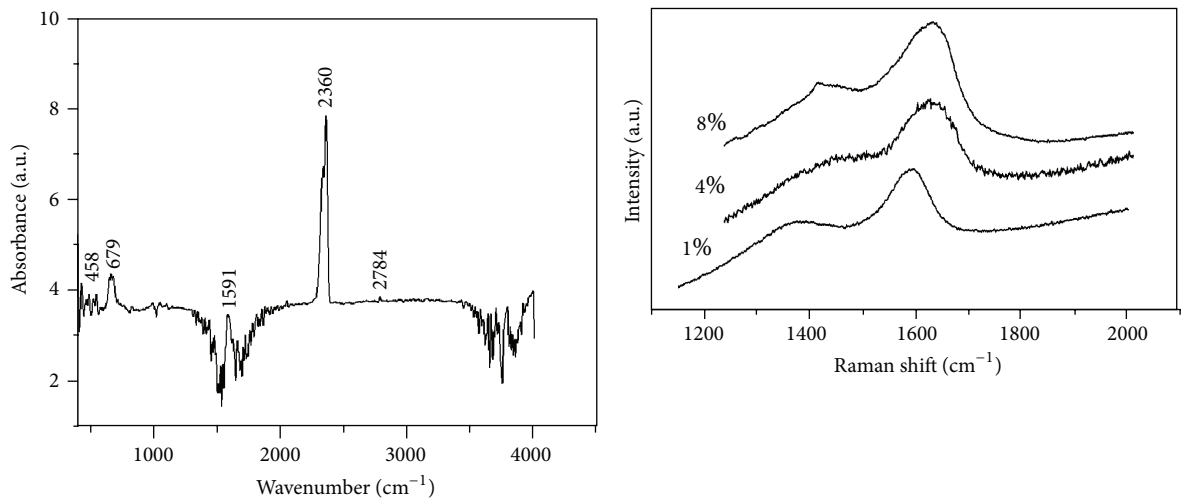

(a) (b)

Figure 2: (a) FTIR spectra for a representative film deposited in a bath containing 1% (v/v) of CH_3COOH. (b) Raman spectra of some representative DLC film deposited in a bath containing different amount of CH_3COOH.

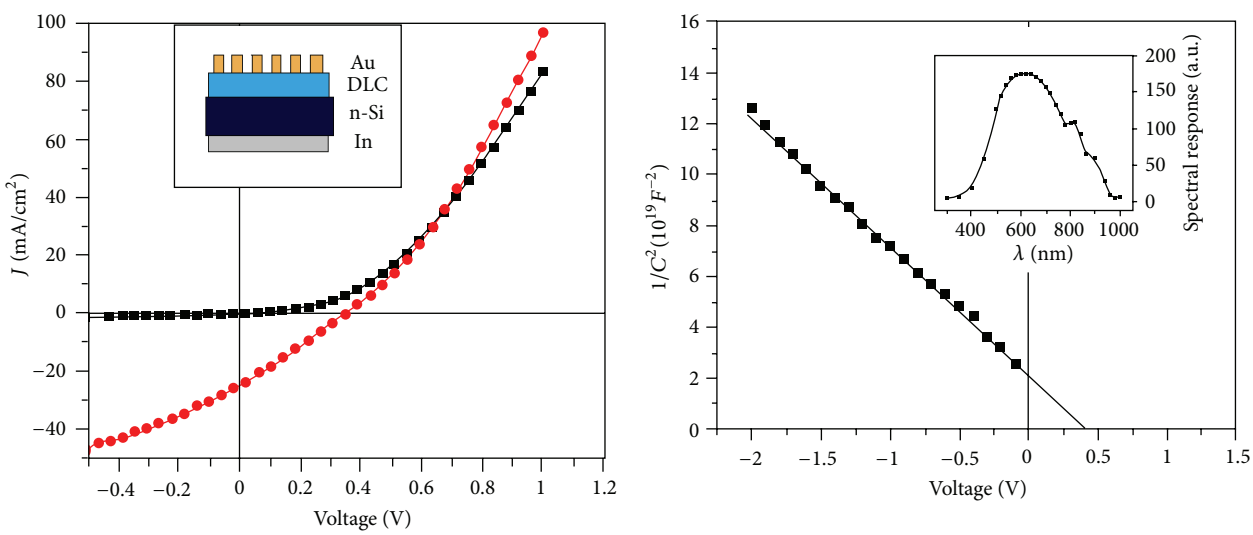

(a) (b)

Figure 3: (a) J-V characteristics (inset shows the schematic diagram) and (b) Mott-Schottky plot (inset shows the spectral response) of a typical cell based n-Si/DLC using the electrolyte as 1% (v/v) CH_3COOH concentration.

A representative cell structure is shown in the inset of Figure 3(a). Figure 3(a) shows the current-voltage curves in the dark and under simulated illumination (60 mW/cm^2). Table 1 shows the photovoltaic parameters (V_{oc}, J_{sc}, FF, η, R_{sh}, R_s) of n-Si/DLC heterojunction fabricated with DLC films deposited with different concentration of CH_3COOH. The cell with the best efficiency was fabricated by applying a constant voltage of 16 V for 1 hour using an electrolyte containing 1% v/v CH_3COOH. An efficiency of 3.7%, with short-circuit current density (J_{sc}) of 24.5 mA/cm^2 and an open-circuit voltage (V_{oc}) of 0.342 V, was recorded for the above cell. These values are superior to those reported by Krishna et al. [11] for n-Si/p-C cells. The cells had poor fill factor. It may be inferred that cells fabricated with optimized layer thicknesses using a bi-layers structure for the window layer would yield more efficient carbon-based solar cells.

C-V characteristic of a representative cell is shown in Figure 3(b). Variation of capacitance with voltage may be expressed as

$$\frac{1}{C^2} = \frac{2(V_{bi} - V)}{qNdK_s\varepsilon_0 A^2}, \tag{2}$$

were q is the electron charge, K_s is the semiconductor dielectric constant, ε_0 is the permittivity of free space, A is the surface area of the solar cell, N_d is the density of donors, and V_{bi} is the built in potential. Equation (2) suggests that $1/C^2$-V plot (Mott-Schottky plot) would be a straight line. N_d could

Table 1: Deposition conditions of DLC films and Cell parameters.

Cell No.	Conc. (% Vol.)	Applied volt (V)	Deposition time (min)	V_{oc} (mV)	J_{sc} (mA/cm^2)	η (%)	FF
1	1	16	60	342	24.5	3.7	0.28
2	4	16	60	350	12.5	1.5	0.21
3	8	16	60	220	1	0.1	0.16
4	1	16	30	225	3	0.1	0.14
5	1	16	90	205	0.95	0.05	0.15

be obtained from the slope of this Mott-Schottky plot. Thus, N_d may be expressed as

$$N_d = \frac{2}{\left[qK_s\varepsilon_0 A^2 \left\{d\left(1/C^2\right)/dv\right\}\right]}. \quad (3)$$

Using the above equation the density of donors (N_d) and built in potential (V_{bi}) were computed from the slope and the intercept of the linear portion of $1/C^2$-V plots. Straight line $1/C^2$-V plots indicated the presence of a sharp interface at the junction. The computed values of the density of donors (N_d) and built-in potential (V_{bi}) for the cell of maximum efficiency were ~6.92×10^{16} cm^{-3} and 0.41 V, respectively. Inset of 3b shows spectral response of solar cell which indicated good blue absorption in the visible range which decreased in the NIR range. A relatively sharp spectral response could be observed for these n-Si/DLC cells with a peak maximum more towards the lower wavelength (around 600 nm). This cell also showed a broad distribution over a wide range of wavelengths from 450 nm to 1000 nm as compared to that reported by Krishna et al. [11] for p-C/n-Si cells.

3.4.2. Open-Circuit Voltage Decay Measurement. The lifetime of photo-generated excess minority carriers is an important parameter in solar-cell design. The overall energy conversion efficiency of a photovoltaic cell critically depended on the base region minority carrier lifetime of the cell. Following Gossick [23], the open-circuit voltage (V_{oc}) decay technique was utilized to determine the minority carrier life time. Gossick's technique involves creating excess minority carriers in a junction device using an external excitation provided by a brief forward current, and then monitoring V_{oc} after the excitation has been abruptly terminated. Minority carrier lifetime can be determined by analyzing the resultant V_{oc} decay curve.

Upon illumination free electrons and holes are generated and separated by the potential barrier of the p-n junction thus an open-circuit voltage has been developed across the junction. When the illumination is switched off, the excess carrier concentration is decreased due to the electron and hole recombination. The decrease can be understood by the following equation [24, 25]:

$$\frac{dn}{dt} = -R = -\frac{n - n_0}{\tau}. \quad (4)$$

n_0 and n are the equilibrium and nonequilibrium electron concentrations in the region of p-type conductivity. t and τ are the time and the carrier lifetime, respectively. R is

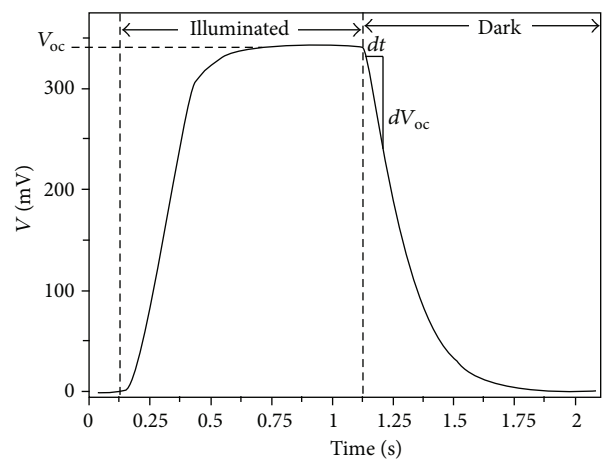

Figure 4: Optical response curve of the cell based on n-Si/DLC structure (1% (v/v) CH_3COOH conc.) using the light of 1 second pulse duration and 60 mW/cm^2 intensity.

the carrier recombination rate. Commonly R is a nonlinear function of n and it can be presented as $R = (n - n_o)/\tau$. Here τ varies nonlinearly with n. The rate at which the open-circuit voltage decays with time would depend on the electron exchange between the conduction and valence bands. The nonequilibrium carrier concentration n has been estimated using the measured open-circuit voltage (V_{oc}) as

$$n = n_0 \exp\left(\frac{qV_{oc}}{\beta kT}\right). \quad (5)$$

Here T is the temperature, k is the Boltzmann constant, and q is the electron charge. β is known as the ideality factor. After the illumination is switched off, V_{oc} decreases with time. The decay transient of V_{oc} has been used to estimate the carrier lifetime [26, 27]. The minority carrier life time could be computed by using the following equation [28]:

$$\tau = \left(\frac{2kT}{q}\right)\left[\frac{1}{(dV_{oc}/dt)}\right]. \quad (6)$$

Figure 4 shows the optical response curve of n-Si/DLC solar cell using the light of 1 second pulse duration and 60 mW/cm^2 intensity. From (6), the estimated carrier life time (τ) was ~ 32 ms.

3.4.3. Impedance Spectroscopy. The real and complex impedances of the device as a function of test frequency

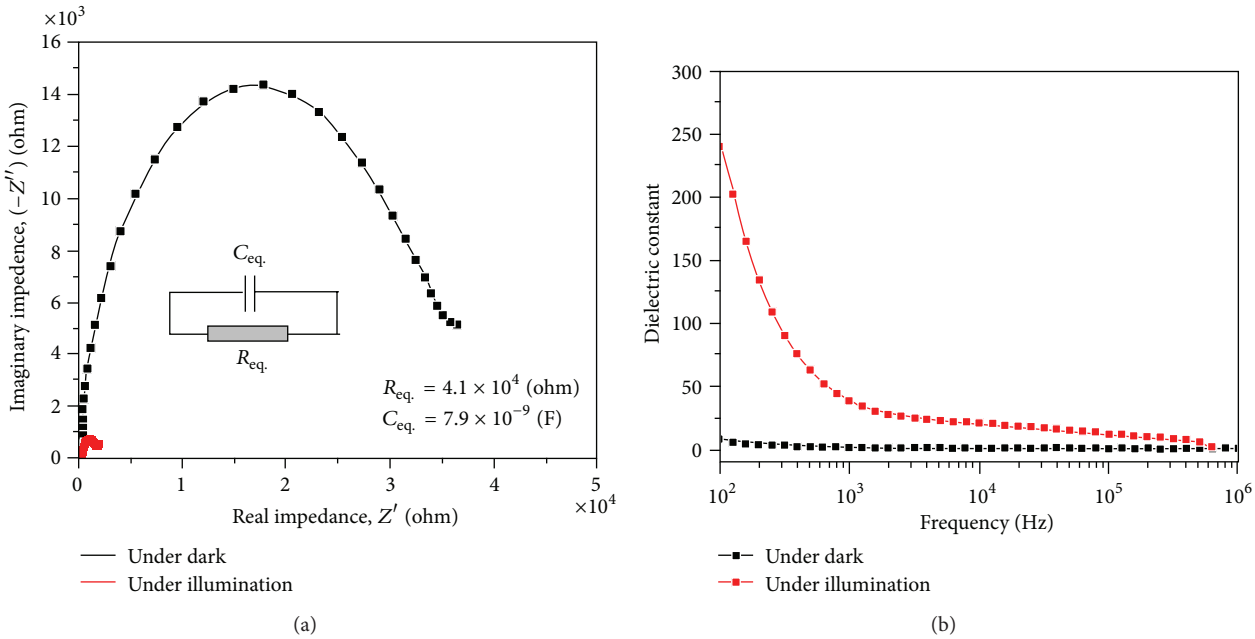

FIGURE 5: (a) Cole-Cole plots between the real (Z') and imaginary (Z'') parts of complex impedance of a device based on n-Si/DLC under dark and 60 mW/cm^2 illumination conditions and (b) dielectric constant versus frequency plots of the complex impedance of a device based on n-Si/DLC under dark and 60 mW/cm^2 illumination conditions.

under dark and illumination conditions were recorded. Photo induced charge separation is associated with an increase in the dielectric constant of the active material and decrease in the device resistance. The relation between the real and imaginary components of impedance, Z' and Z'', respectively, (Cole-Cole plots) is shown in Figure 5(a). The nature of the Cole-Cole plots is one impedance semicircular arc. The nature of the Cole-Cole plots is one impedance semicircular arc. It may be observed that these plots are very nearly semicircular in shape under the zero and reverse bias conditions indicating that the AC equivalent circuit of the solar cell consists of an R and a C in parallel, and the equivalent circuit of the device would consist of a single RC network with a single time constant. With increasing frequency, Z' decreases and Z'' shows a peak at $f_{\max}$ where the semicircular arc is maximum. Thus, the complex impedance plot shows one semicircular arc representing the bulk properties of the grains. The electrical contribution of the grains was introduced by using a simple equivalent circuit with parallel combination of a resistance (R_{eq}) and a capacitor (C_{eq}) with the diameter of the semicircle representing the resistance as shown in Figure 5(a). The capacitance (C_{eq}) was calculated using the relation

$$\omega\tau = 2\pi f_{\max} R_{\text{eq}} C_{\text{eq}} = 1. \tag{7}$$

The capacitance value computed from the above was ~8 × 10^{-9} F.

The Cole-Cole plots for n-Si/DLC device remain semicircular under both dark and illumination. When the device was illuminated, photocurrent flowed through the device and the diameter of the semicircle is reduced. This is due to the semiconducting nature of the active layer in which the resistance decreases with an increase in the applied voltage. The diameter, however, reduced by more than 90% in case of illumination. This large decrease in device resistance upon illumination may assert the presence of free carriers, which appeared due to excitation at different interfaces as well as photo induced electron transfer from bulk Si to DLC.

Frequency dependent capacitance of the device has been modeled as a parallel combination of a resistance and a capacitor (Figure 5(a)). The dielectric constant of the active layer could be obtained from the value of capacitance, area, and thickness of the devices. Figure 5(b) shows the variation of dielectric constant versus frequency plots of a typical device based on n-Si/DLC under dark and illumination conditions. The result shows that the dielectric constant at any frequency increases upon illumination. This increase is due to photo induced electron transfer similar to electrical polarization, which allows more carriers to accumulate at the electrodes during the impedance measurement.

Dielectric relaxation time (τ_{relax}) can be calculated from critical frequency, $f_{\max}$, at which Z'' is maximum obtained from Cole-Cole plot as shown in Figure 5(a). The connection between the dielectric measurement made in frequency domain and that made in time domain is given by the Fourier transform relation expressed as below [29]:

$$\tau_{\text{relax}} = \frac{1}{[2\pi f_{\max}]}. \tag{8}$$

Thus, using the value of $f_{\max}$ from Figure 5(a), the value of τ_{relax} computed was ~50 μS.

4. Conclusion

Diamond-like carbon films were electrodeposited on n-Si substrate to realize an n-Si/DLC PV structure. The films thus obtained were characterized by FESEM, XPS, FTIR, and Raman studies. Two broad peaks, located at 1365 cm^{-1} (D-line) and 1575 cm^{-1} (G-line) constituted the Raman spectra of the DLC films. From impedance spectroscopy, we observed that photoinduced charge separation in n-Si (100)/DLC structure is associated with an increase in the dielectric constant and a decrease in the device resistance. From V_{oc} decay measurement, it was found that upon switching off the illumination, the open-circuit voltage decreased with time according to the exponential function. Maximum efficiency of 3.7% with $V_{oc} \sim 0.34$ V and $J_{sc} \sim 24.5$ mA/cm^2 was obtained for the device based on n-Si (100)/DLC structure. The density of donors ($N_d \sim 6.92 \times 10^{16}$ cm^{-3}) and built in potential ($V_{bi} \sim 0.41$ V) were computed from the slope and the intercept of the linear portion of $1/C^2$-V plots.

Acknowledgments

D. Ghosh and B. Ghosh wish to thank the Department of Science and Technology, Government of India, and UGC-DAE CSR for granting them the fellowships. Thanks are due to Mr. Sudip K. Saha, IACS, Calcutta, for recording the impedance spectra.

References

[1] A. Grill, "Electrical and optical properties of diamond-like carbon," *Thin Solid Films*, vol. 355, pp. 189–193, 1999.

[2] G. Reisel, S. Steinhäuser, and B. Wielage, "The behaviour of DLC under high mechanical and thermal load," *Diamond and Related Materials*, vol. 13, no. 4–8, pp. 1516–1520, 2004.

[3] P. Lemoine, J. P. Quinn, P. D. Maguire, J. F. Zhao, and J. A. McLaughlin, "Intrinsic mechanical properties of ultra-thin amorphous carbon layers," *Applied Surface Science*, vol. 253, no. 14, pp. 6165–6175, 2007.

[4] M. Zhang, Y. Xia, L. Wang, and W. Zhang, "The electrical properties of diamond-like carbon film/D263 glass composite for the substrate of micro-strip gas chamber," *Diamond and Related Materials*, vol. 12, no. 9, pp. 1544–1547, 2003.

[5] C. H. Su, C. R. Lin, C. Y. Chang, H. C. Hung, and T. Y. Lin, "Mechanical and optical properties of diamond-like carbon thin films deposited by low temperature process," *Thin Solid Films*, vol. 498, no. 1-2, pp. 220–223, 2006.

[6] E. Martínez, J. L. Andújar, M. C. Polo, J. Esteve, J. Robertson, and W. I. Milne, "Study of the mechanical properties of tetrahedral amorphous carbon films by nanoindentation and nanowear measurements," *Diamond and Related Materials*, vol. 10, no. 2, pp. 145–152, 2001.

[7] Z. Gan, Y. Zhang, G. Yu, C. M. Tan, S. P. Lau, and B. K. Tay, "Intrinsic mechanical properties of diamond-like carbon thin films deposited by filtered cathodic vacuum arc," *Journal of Applied Physics*, vol. 95, no. 7, pp. 3509–3515, 2004.

[8] H. Zhu, J. Wei, K. Wang, and D. Wu, "Applications of carbon materials in photovoltaic solar cells," *Solar Energy Materials and Solar Cells*, vol. 93, no. 9, pp. 1461–1470, 2009.

[9] M. Bernard, J. Lohrman, P. V. Kumar et al., "Nanocarbon-based photovoltaics," *ACS Nano*, vol. 6, pp. 8896–8903, 2012.

[10] N. I. Klyui, O. B. Korneta, V. P. Kostylyov et al., "High efficient solar cells and modules based on diamond-like carbon films-multicrystalline Si structures," *Semiconductor Physics, Quantum Electronics & Optoelectronics*, vol. 6, pp. 197–201, 2003.

[11] K. M. Krishna, M. Umeno, Y. Nukaya, T. Soga, and T. Jimbo, "Photovoltaic and spectral photoresponse characteristics of n-C/p-C solar cell on a p-silicon substrate," *Applied Physics Letters*, vol. 77, no. 10, pp. 1472–1474, 2000.

[12] R. K. Roy, S. Gupta, B. Deb, and A. K. Pal, "Electron field emission properties of electro-deposited diamond-like carbon coatings," *Vacuum*, vol. 70, no. 4, pp. 543–549, 2003.

[13] R. K. Roy, B. Deb, B. Bhattacharjee, and A. K. Pal, "Synthesis of diamond-like carbon film by novel electrodeposition route," *Thin Solid Films*, vol. 422, no. 1-2, pp. 92–97, 2002.

[14] R. Paul, S. Dalui, S. N. Das, R. Bhar, and A. K. Pal, "Hydrophobicity in DLC films prepared by electrodeposition technique," *Applied Surface Science*, vol. 255, no. 5, pp. 1705–1711, 2008.

[15] S. Gupta, M. P. Chowdhury, and A. K. Pal, "Field emission characteristics of diamond-like carbon films synthesized by electrodeposition technique," *Applied Surface Science*, vol. 236, no. 1, pp. 426–434, 2004.

[16] P. Avouris and R. Martel, "Progress in carbon nanotube electronics and photonics," *MRS Bulletin*, vol. 35, no. 4, pp. 306–313, 2010.

[17] V. C. Tung, J. H. Huang, J. Kim, A. J. Smith, C. W. Chu, and J. Huang, "Towards solution processed all-carbon solar cells: a perspective," *Energy & Environmental Science*, vol. 5, pp. 7810–7818, 2012.

[18] K. P. Loh, Q. Bao, G. Eda, and M. Chhowalla, "Graphene oxide as a chemically tunable platform for optical applications," *Nature Chemistry*, vol. 2, no. 12, pp. 1015–1024, 2010.

[19] L. H. Yang, C. Y. Fong, and C. S. Nichols, *Fall Meeting of the Materials Research Society*, Boston, Mass, USA, 1990.

[20] A. Grill and V. Patel, "Characterization of diamondlike carbon by infrared spectroscopy," *Applied Physics Letters*, vol. 60, no. 17, pp. 2089–2091, 1992.

[21] J. R. Dyer, *Application of Absorption Spectroscopy of Organic Compounds*, Prentic-Hall, New Delhi, India, 2002.

[22] A. C. Ferrari and J. Robertson, "Interpretation of Raman spectra of disordered and amorphous carbon," *Physical Review B*, vol. 61, no. 20, pp. 14095–14107, 2000.

[23] B. R. Gossick, "On the transient behavior of semiconductor rectifiers," *Journal of Applied Physics*, vol. 26, no. 11, pp. 1356–1365, 1955.

[24] A. B. Walker, L. M. Peter, K. Lobato, and P. J. Cameron, "Analysis of photovoltage decay transients in dye-sensitized solar cells," *Journal of Physical Chemistry B*, vol. 110, no. 50, pp. 25504–25507, 2006.

[25] A. Zaban, M. Greenshtein, and J. Bisquert, "Determination of the electron lifetime in nanocrystalline dye solar cells by open-circuit voltage decay measurements," *ChemPhysChem*, vol. 4, no. 8, pp. 859–864, 2003.

[26] T. Pisarkiewicz, "Photodecay method in investigation of materials and photovoltaic structures," *Opto-Electronics Review*, vol. 12, no. 1, pp. 33–40, 2004.

[27] V. Kveder, M. Badylevich, E. Steinman, A. Izotov, M. Seibt, and W. Schröter, "Room-temperature silicon light-emitting diodes based on dislocation luminescence," *Applied Physics Letters*, vol. 84, no. 12, pp. 2106–2108, 2004.

[28] E. M. John, W. E. Thomas, I. F. Robert, and K. Roy, "Measurement of minority carrier life time in solar cells from photo-induced open circuit voltage decay," *IEEE Transactions on Electron Devices*, vol. 26, no. 5, 1979.

[29] H. J. Choi, C. H. Hong, and M. S. Jhon, "Cole-Cole analysis on dielectric spectra of electrorheological suspensions," *International Journal of Modern Physics B*, vol. 21, no. 28-29, pp. 4974–4980, 2007.